Multivariate pattern analysis reveals resting-state EEG biomarkers in fibromyalgia

Dino Soldic[1,3], María Carmen Martín-Buro[1,3], David López-García[2], Ana Belén del Pino[1,3], Roberto Fernandes-Magalhaes[1,3], David Ferrera[1,3], Irene Peláez[1,3], Luis Carretié[4], and Francisco Mercado[1,3]

Author affiliations:

1 Department of Psychology, Faculty of Health Sciences, Rey Juan Carlos University, 28922 Alcorcón, Madrid, Spain

2 Mind, Brain and Behavior Research Center, 18011 Granada, Andalucía, Spain.

3 Research group in Cognitive Neuroscience, Pain and Rehabilitation (NECODOR), Rey Juan Carlos University, 28922 Alcorcón, Madrid, Spain

4 Faculty of Psychology, Autonomous University of Madrid, 28049 Madrid, Spain

Correspondence to: Francisco Mercado

Department of Psychology, Faculty of Health Sciences, Rey Juan Carlos University, 28922 Alcorcón, Madrid, Spain

E-mail: francisco.mercado@urjc.es

Keywords: chronic pain; neural markers; multivariate analysis; decoding; support vector machine; discriminant analysis

Abstract

Fibromyalgia (FM) involves widespread musculoskeletal pain and hypersensitivity, often accompanied by neurological, cognitive, and affective disturbances. Resting-state (RS) electroencephalography (EEG) studies have revealed abnormal brain activity in chronic pain conditions, with anxiety and symptom duration potentially exacerbating these alterations. This study applied multivariate pattern analysis to differentiate RS-EEG signals between FM patients and healthy controls across frequency bands associated with pain processing, incorporating state and trait anxiety scores. It also examined differences between patients with short and long duration symptoms and identified the most relevant scalp regions contributing to the models. Fifty-one female participants (25 FM patients, 26 controls; aged 35-65) were included. Patients were classified into short-term (12) and long-term (13) groups. Normalized power spectral density values were extracted from EEG data and used to train machine learning classifiers, with Haufe-transformed weights computed to determine key scalp contributions. The models distinguished patients from controls with accuracies exceeding 0.70 across all frequency bands, reaching 0.99 in beta and gamma bands when anxiety was included. Symptom duration was also a relevant factor, as the model differentiated short- from long-term FM patients with accuracies up to 0.96 in beta and gamma bands. Alterations in theta power within frontal and parietal regions, along with frequency-specific contributions, highlight disrupted pain processing in FM and suggest cumulative effects of prolonged symptom duration. RS-EEG combined with multivariate pattern analysis may support the development of biomarkers to improve diagnosis and guide treatment strategies in clinical settings.

1 Introduction

Fibromyalgia (FM) affects 2-8% of the population, predominantly women [11]. The syndrome is characterized by widespread musculoskeletal pain and hypersensitivity, also affecting neurological, cognitive, and affective domains [17,20,21,25,48,49]. As a nociplastic pain syndrome [12,22], FM presents a controversial neurobiological basis and highly variable comorbid symptoms (e.g., fatigue and insomnia), which complicate both diagnosis and treatment despite established criteria [38,61,62]. These challenges have prompted researchers to record electromagnetic brain signals to better understand its underlying mechanisms. Electroencephalography (EEG) is especially useful, as it can detect abnormalities in basal brain function even during resting-state (RS) conditions. In this line, anomalous cortical activity in FM has been shown to be more concentrated in parietal regions within theta, alpha, and beta bands [42]. Additionally, Fallon et al. [17] observed increased theta activity associated with heightened pain perception, localized via source reconstruction to the anterior cingulate, medial prefrontal, and dorsolateral prefrontal cortices. Other studies report diminished connectivity between default mode network regions and somatosensory cortices in the theta band [10,33], a pattern linked to hypersensitive neural processing in FM [42]. Complementing these findings, González-Villar et al. [26] observed increased alpha and beta activity in frontal regions, possibly reflecting dysregulated top-down control contributing to FM patients' attentional and cognitive deficits [18,19].

Among the factors that may influence these alterations, symptom duration is particularly relevant. Continuous nociceptive input, characteristic of chronic pain conditions, appears to alter processing in cortical regions [3,5,35,51], reduce deactivations, and disrupt inhibitory interactions between the dorsolateral and medial prefrontal cortices [4]. Similar patterns have been observed in FM, with several studies linking symptom duration to increased theta power in frontal and parietal regions, suggesting that prolonged exposure to pain and leads to

progressive alterations in FM [59]. Furthermore, frontocentral activity changes associated with ongoing tonic pain and fatigue support the notion of a cumulative neural impact with prolonged FM exposure [2,17]. However, chronic pain is not only a defining feature of FM but may also be influenced by other comorbid symptoms, particularly affective factors [30]. Anxiety is among the most prevalent affective symptoms in FM [23] and often leads to a marked reduction in quality of life [8,9]. Notably, it has been associated with altered cortical baseline processing, with trait anxiety linked to disrupted activity within the default mode network and its connections to frontal regions, and state anxiety related to both the salience and default mode networks [53].

Given the syndrome's variability and complexity, machine learning (ML) methods have gained popularity for their ability to improve statistical sensitivity and specificity by detecting subtle signal changes often overlooked by conventional analyses, thereby preserving valuable information [39,41,57,65]. For instance, López-Solà et al. [40] identified new cortical regions involved in FM using multivariate pattern analysis of functional magnetic resonance imaging data. Furthermore, Hsiao et al. [32] employed a multivariate ML model to predict individual differences in heat pain sensitivity, combining RS-EEG features such as power spectral density, functional connectivity, and psychometric metrics. Their study demonstrated that combining neurophysiological and neuropsychological variables enhances predictive performance, highlighting the utility of ML in uncovering underlying neural mechanisms based on RS-EEG features [1].

Despite their potential, such approaches have yet to be systematically applied to FM populations, highlighting the need for methods that deepen our understanding of FM's neurobiological foundations and reliably differentiate patients from HC, while accounting for clinical symptoms. Therefore, this study aims to: 1) differentiate RS-EEG signals of FM patients and HC across frequency bands leveraging state and trait anxiety scores; 2)

distinguish patients based on symptom duration; and 3) identify neural activity in key scalp regions contributing to classification.

2 Materials and methods

2.1 Paradigm and data acquisition

2.1.1 Participants

Fifty-one women participated in the study, comprising 25 fibromyalgia (FM) patients (mean age ± SD = 52.15 ± 6.06) and 26 healthy controls (HC; mean age ± standard deviation [SD] = 48.73 ± 7.01), with ages ranging from 35 to 65 years. FM patients were recruited through the Fibromyalgia and Chronic Fatigue Syndrome Association of Móstoles (AFINSYFACRO) and the Madrid Fibromyalgia Association (AFIBROM). They were evaluated by rheumatologists from hospitals in the Community of Madrid and met the diagnostic criteria defined by the American College of Rheumatology [61,63]. HC were recruited through posters displayed around the Faculty of Health Sciences at Rey Juan Carlos University, as well as through emails sent to the entire university community. Participants with neurological disorders, metabolic alterations, cognitive impairments, substance abuse or dependence, or psychiatric disorders were excluded from the study. FM patients had a mean diagnosis duration of 94 months (SD = 50.77). Prescribed medications and therapeutic interventions were continued due to medical recommendations and ethical guidelines. Group differences in age and anxiety scores between FM and HC participants were assessed using two-tailed independent-samples *t*-tests with a 95% confidence interval, while differences in educational level were evaluated using a chi-square (χ^2) test.

2.1.2 Procedure

The study adhered to the ethical standards of the World Medical Association's Helsinki Declaration (1964) and its later amendments. All participants provided written informed consent, and the study was approved by the Rey Juan Carlos University Research Ethics Committee (ref: 201000100011550).

Upon arrival at the Laboratory of Cognitive Neuroscience (Faculty of Health Sciences, Rey Juan Carlos University), participants completed a sociodemographic and clinical questionnaire. Sociodemographic data included age, educational level, and regular medication use. Additionally, FM patients reported the duration of their diagnosis in months. FM and HC groups were matched for age [t (49) = 1.625, p = 0.111, d = 0.455] and educational level [$\chi^2(4) = 8.106$, p = 0.088, V = 0.399]. To assess both state (STAI-S) and trait (STAI-T) anxiety the State-Trait Anxiety Inventory (STAI) [55] was administered. Sociodemographic and clinical data are presented in Table 1.

Table 1 Sociodemographic and clinical data

	Fibromyalgia (*N* = 25)	**Healthy Control (*N* = 26)**	***T*-test/ chi square**	**Significance level**	**Effect size**
Age (years. M ± SD)	51.60 ± 5.47	48.73 ± 7.01	t = 1.625	p = 0.111	d = 0.455
Educational level			χ^2 = 8.106	p = 0.088	V = 0.399
None, *N* (%)	3 (5.9%)	0 (0%)	-	-	-
Primary school, *N* (%)	11 (21.6%)	8 (15.7%)	-	-	-
Secondary school, *N* (%)	7 (13.7%)	6 (11.8%)	-	-	-
High school, *N* (%)	3 (5.9%)	11 (21.6%)	-	-	-
Bachelor's degree, *N* (%)	1 (2%)	1 (2%)	-	-	-
Diagnosis history (months. M ± SD)	94 ± 50.77	-	-	-	-
Diagnosis history (months. Median)	92	-	-	-	-
Medication					
Antidepressants, *N* (%)	14 (56%)	0 (0%)	-	-	-
Anxiolytics, *N* (%)	6 (24%)	0 (0%)	-	-	-
Analgesics, *N* (%)	10 (40%)	0 (0%)	-	-	-
Antiepileptics/Psycholeptics, *N* (%)	4 (16%)	0 (0%)	-	-	-
Other, *N* (%)	9 (36%)	0 (0%)	-	-	-
Trait anxiety (STAI-T percentile. M ± SD)	81.94 ± 19.33	29.73 ± 27.96	t = 7.781	p < 0.001	d = 2.172
State anxiety (STAI-S percentile. M ± SD)	60.52 ± 26.48	15.77 ± 18.94	t = 6.918	p < 0.001	d = 1.944

Abbreviations: N = Sample size; M = Mean; SD = Standard deviation.

2.1.3 EEG data acquisition and preprocessing

EEG recording took place in a room fully equipped to minimize noise, electromagnetic interference, and environmental influences, providing an optimal setting for the procedure. Continuous EEG activity was recorded from 60 homogeneously distributed electrodes (10-10 system) mounted on a cap (ElectroCap International), referenced to both mastoids. Vertical and horizontal eye movements were monitored through electrooculographic (EOG) recordings. The vertical EOG electrodes were positioned both below and above the left eye orbit, while the horizontal EOG electrodes were situated on the left and right orbital rims. Electrode impedances were maintained below 5 kΩ, and a bandpass filter of 0.1 – 50 Hz (3 dB points for -6 dB/octave roll-off) was applied to the recording amplifiers. Data were continuously digitized at a sampling rate of 250 Hz. Offline preprocessing was performed using a custom MATLAB R2023b [43] script containing EEGLAB v2023.1 [15] functions.

The EEG dataset used in this study was recorded as a part of a broader investigation involving event-related potentials (ERP), which falls beyond the scope of this article. In that experiment, participants were asked to perform a simple visual task that required categorizing a central digit as either above or below five, while peripheral stimuli were simultaneously presented (see, for example, Carretié [7]). Visual stimuli were displayed for 50 ms, with an interstimulus interval (ISI) of 3000 ms. During the ISI, participants stared at a fixation cross without engaging in any other activity. Previous studies described that ERPs can last up to 900 ms post-stimulus onset gradually returning to baseline cortical activity [34]. Meanwhile, during attentional tasks, activity in the default mode network increases greatly around 600 ms upon stimulus onset and around 200 ms after the response [60], reflecting a transition to RS brain activity [50]. Thus, to define EEG segments free from task-related activity (i.e., RS signal), the maximum response time across all participants (850 ms) in the ERP paradigm was extracted, and an additional 500 ms latency was added. Epochs were then defined from

1350 ms after stimulus onset to 300 ms before the next stimulus onset. This resulted in a total of 4893 RS epochs with eyes open, each lasting 1350 ms, as per previous studies [14,17]. Prior to epoching, ocular channels were removed from the data, and the entire EEG recordings were digitally filtered using a zero-phase finite impulse response (FIR) filter implemented in EEGLAB's *pop_eegfiltnew* function (0.5-50 Hz), with default filter order and transition bandwidth parameters. Eye blink artifacts were removed from the epoched data using Independent Component Analysis through EEGLAB's *runica* algorithm. Out of 60 total components, an average of 1 component (*SD* = 0.4) was removed for the HC group and 1.31 components (*SD* = 0.61) were removed for the FM group. No channels needed to be interpolated for any participant. To prune epochs containing artifacts, a semi-automatic trial rejection was performed based on voltage thresholds set at ± 100 μV. To further ensure there was no lingering task activity in the data, epochs that still contained a response event were manually selected and removed. As a result, an average of 94.04 epochs (*SD* = 1.89) for the FM group and 94.42 epochs (*SD* = 2.86) for the HC group were retained for subsequent analyses. After artifact removal the data were re-referenced to the common average reference. The MATLAB script used for preprocessing is available at: https://github.com/dinosoldic/EEG-Preproc-ERP/blob/main/eegPreproc.m. A summary of the EEG analysis pipeline is presented in Figure 1.

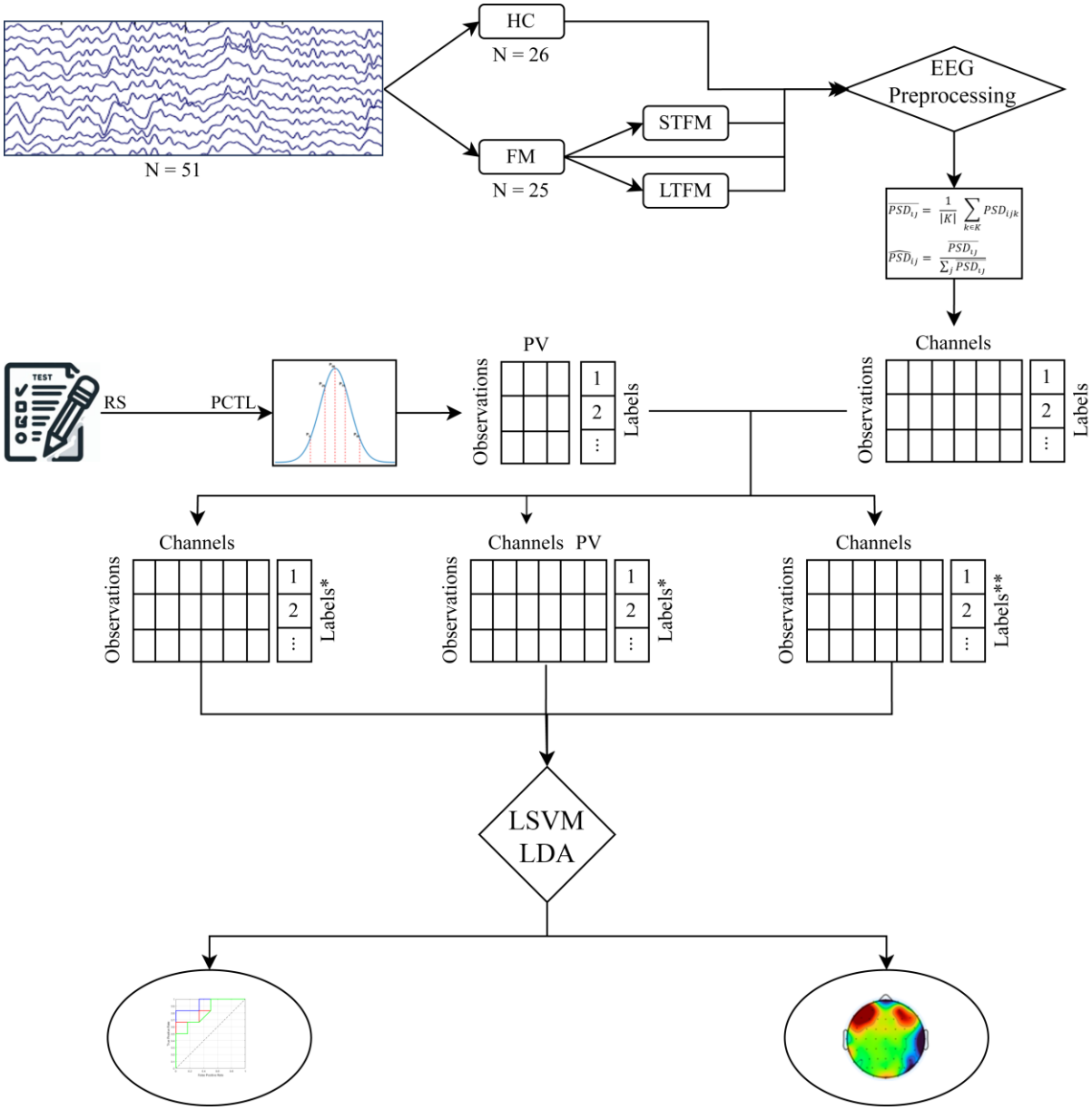

Figure 1 Pipeline of data processing and analyses. (*) indicates labels used for FM and HC comparison. (**) indicates labels used for STFM and LTFM comparison. Abbreviations: N = Sample size; HC = Healthy controls; FM = Fibromyalgia; STFM = Short-term fibromyalgia; LTFM = Long-term fibromyalgia; EEG = Electroencephalography; RS = Raw scores; PCTL = Percentile; PV = Psychometric values; LSVM = Linear support vector machine; LDA = Linear discriminant analysis.

2.2 Feature extraction

Building on previous studies examining RS data and patient diagnosis [1,32,52], the EEG data was decomposed into frequency bands. The resulting bands were as follows: delta (2 – 3.5 Hz), theta (4 – 7.5 Hz), alpha (8 – 12 Hz), alpha-1 (8 – 10 Hz), alpha-2 (10 – 12 Hz), beta (13 – 30 Hz), beta-1 (13 – 18 Hz), beta-2 (18.5 – 21 Hz), beta-3 (21.5 – 30 Hz), and gamma

(30.5 – 44 Hz) [17,58]. These frequency bands were obtained using the *ft_freqanalysis* function in FieldTrip [47], applying the multitaper method for fast Fourier transform (mtmfft) with discrete prolate spheroid sequences on frequencies of interest ranging from 0.5 to 50 Hz, spaced at 0.74 Hz.

Once extracted, power spectral density (PSD) values were averaged across bins within each frequency band (Equation 1), and normalized (Equation 2) by dividing the PSD value at each channel by the total power of its corresponding observation [32]. This procedure was applied separately to each frequency band.

$$\overline{PSD_{ij}} = \frac{1}{|K|} \sum_{k \in K} PSD_{ijk} \quad (1)$$

$$\widehat{PSD}_{ij} = \frac{\overline{PSD_{ij}}}{\sum_j \overline{PSD_{ij}}} \quad (2)$$

In addition to the frequency bands, psychometric values (PV) were extracted from self-reported anxiety scores obtained through the STAI questionnaire. These values consisted of the percentile scores for each participant on both the trait and state anxiety scales. Prior to being used as additional features, these values were tested for significance between groups (Table 1) and trained separately from the PSD values. Significant PV were added as features along with PSD to examine their potential contribution to classification performance and to assess whether anxiety-related measures provide additional discriminative power between groups. Since PSD and PV are measured in different units, they were normalized using the *zscore* function in MATLAB. Consequently, the training and testing datasets for comparing HC and FM were constructed using PSD, PV (STAI-S, STAI-T, and STAI-S + STAI-T), as well as combinations of PSD and PV (PSD + STAI-S, PSD + STAI-T, and PSD + STAI-S + STAI-T).

Additionally, the FM group was divided into two subgroups based on diagnostic length: 12 patients were included in the short-term fibromyalgia (STFM) group and 13 in the long-term fibromyalgia (LTFM) group. The median diagnostic length (92 months, $Q1$ = 64, $Q3$ = 107) served as the cutoff, with participants at the median value being randomly assigned to either group to ensure balance. As a result, a training and testing dataset was constructed using the PSD values from both groups to compare STFM and LTFM. To control for potential medication effects on brain activity within the FM group, a nonparametric permutation test was applied, given the small sample sizes and non-normal data distribution. Group-averaged PSD values were used for each channel and frequency band, with significance assessed via 5000 permutations and Monte Carlo p-values [41].

2.3 Classification models and performance evaluation

To distinguish between FM and HC, as well as between STFM and LTFM, linear discriminant analysis (LDA) and linear support vector machine (LSVM) models were trained. LSVM was defined using MATLAB's *fitcsvm* function with a linear kernel, automatic kernel scaling, box constraint set to 1, and standardized predictors. LDA was built using MATLAB's *fitcdiscr* with a linear discriminant type, no regularization (Gamma = 0), and fill coefficients enabled. Class names were explicitly specified in both models to ensure consistent label mapping. These models have previously been considered particularly well-suited for EEG decoding in cognitive neuroscience [24,54]. This is due to their simplicity, high computational efficiency, and ability to handle high-dimensional data [13,64]. Moreover, they exhibit high robustness to noise, which is especially useful since EEG data, even after preprocessing, tend to contain leftover noise signals [36].

Following PROBAST+AI guidelines [45], model performance was evaluated using accuracy (ACC), area under the receiver operating characteristic curve (AUC), recall, precision, F1-

score, and calibration intercept and slope. Calibration was assessed following the weak calibration procedure described Van Calster et al. [46]. To mitigate potential overfitting, ten-fold cross-validation was employed. In this procedure, the dataset is split into ten subsets (folds). In each iteration, one fold serves as the test set while the remaining nine are used for training. This process is repeated ten times so that each fold is used once for testing, and the performance metrics are then averaged across folds to obtain a robust estimate. Additionally, to account for data variability and assess the stability of the performance metrics, the cross-validation procedure was repeated 1000 times, and mean values were reported. As a baseline comparison, models were also trained on data with randomly permuted class labels. Given the relatively small sample size, no participants were reserved for external validation. However, in accordance with PROBAST+AI recommendations, this does not necessarily indicate a high risk of bias, provided that internal validation is rigorous and appropriately implemented. Overall judgment of prediction model was labeled as low across all four domains: development quality and applicability concern, and evaluation risk of bias and applicability concern. Full assessment is described in Supplementary Table 1. Finally, a two-tailed paired-samples *t*-test with a 95% confidence interval was conducted to compare the classification performance of the LSVM and LDA models, in order to determine the most suitable approach.

2.4 Channel contribution analysis

Since our focus was on linear model variants, the weight of each channel after training can be interpreted as its contribution to the model's performance [29]. However, these weights should not be treated as straightforward indicators of brain activity since a channel with a large weight does not necessarily indicate the presence of the signal of interest, and a channel with a small weight may still carry relevant information [6,29]. To improve interpretability,

the weight vectors were corrected using the method proposed by Haufe et al. [29], allowing them to be more accurately understood as sources of neural activity in space [39]. Furthermore, given that we considered the FM and STFM groups as true positive and the HC and LTFM groups as true negative in their respective analyses, positive weights indicate a higher contribution of a particular channel to correctly classify an observation as FM or STFM, while negative weights would reflect a greater contribution to classifying it as HC or LTFM.

3 Results

3.1 PSD spatial distribution differences

As described in the methods section, power spectral density (PSD) values were averaged within each group, and group-level difference (FM - HC and STFM - LTFM) maps were computed to explore spatial patterns prior to model input. The resulting spatial distributions are illustrated in Figure 2 and further detailed in Supplementary Tables 2 and 3. Relative to the HC group, the FM group showed a tendency toward concentrated activity in prefrontal regions across delta, theta, and alpha bands, as well as in prefrontal and right occipitotemporal areas for beta and gamma bands. In contrast, the HC group appeared to show concentrated activity in left frontotemporal and right frontal regions in beta and gamma bands. Furthermore, the STFM group's activity appeared concentrated in prefrontal regions across all frequency bands, in the left frontotemporal region for delta, and in frontocentral and right frontal regions for beta and gamma bands. Meanwhile, the LTFM group's activity was localized around occipitotemporal regions from delta to beta bands, and in left frontotemporal and right temporal regions for beta and gamma bands.

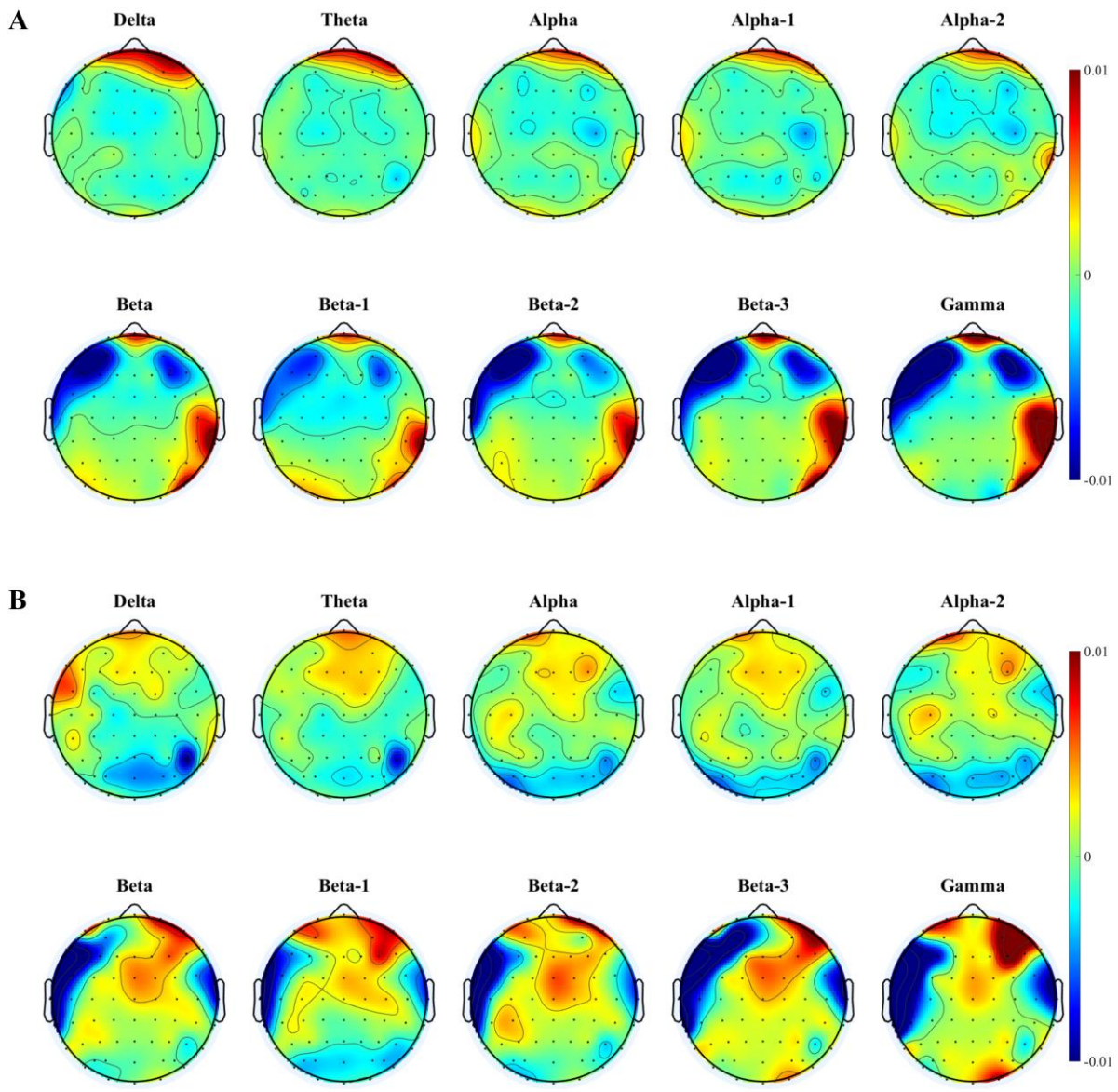

Figure 2 Topographic representation of scalp sites across frequency bands. (**A**) Differences in normalized PSD between FM and HC. (B) Differences in normalized PSD between STFM and LTFM.

3.2 Model performance

To identify the most suitable model for distinguishing patients from controls based on power spectral density (PSD) values, both linear discriminant analysis (LDA) and linear support vector machine (LSVM) models were trained across frequency bands. A paired *t*-test revealed that LSVM significantly outperformed LDA ($p < 0.001$) in delta, theta, beta, beta-2,

beta-3, and gamma bands, whereas LDA showed superior performance in alpha, alpha-1, alpha-2, and beta-1 bands. However, based on calibration scores, LDA demonstrated significantly greater overall stability, with slope values closer to 1 and intercept values closer to 0, except for the slope in the delta band and intercepts in beta-3 and gamma bands. Thus, LDA was selected for subsequent analyses. Performance metrics are illustrated in Figure 3 and further detailed in Supplementary Table 4.

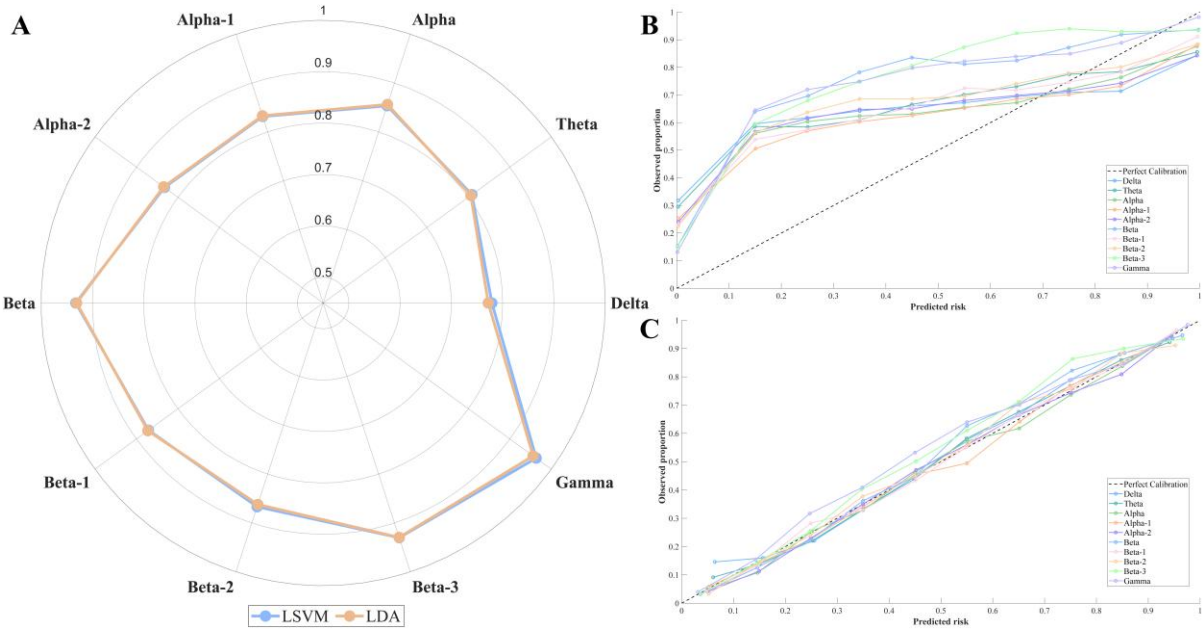

Figure 3 Classifier performance. (**A**) Classifier discrimination performance (AUC) across frequency bands using PSD values for LDA and LSVM models. Calibration curves per frequency band for (**B**) LSVM and (**C**) LDA.

3.3 Classification using discriminative features of EEG data

3.3.1 EEG features and anxiety scores in FM classification

To distinguish HC from FM, power spectral density (PSD) from EEG data and psychometric values (PV) from the STAI questionnaire were used to train a linear discriminant analysis (LDA) model. Performance across feature combinations is shown in Figure 4 and detailed in Supplementary Table 5. The permuted label accuracy was approximately 0.5 for all frequencies, confirming the validity of the data. With PSD alone the model distinguished well

between groups, particularly in beta-3 (*ACC* = 0.86, *AUC* = 0.93) and gamma (*ACC* = 0.89, *AUC* = 0.96) bands. Including either state (PSD + STAI-S) or trait (PSD + STAI-T) anxiety further improved performance across all bands, achieving AUC values above 0.99 for both beta-3 and gamma bands. The best distinction was obtained by combining all features, especially in beta-3 (*ACC* = 0.97, *AUC* = 1.00) and gamma (*ACC* = 0.98, *AUC* = 1.00). On the other hand, the calibration curves were relatively stable and close to the ideal diagonal line when using PSD alone, whereas the inclusion of PV led to greater deviations from perfect calibration, indicating over-confidence in the predicted probabilities for PSD + STAI-S, and under-confidence for PSD + STAI-T and PSD + STAI-S + STAI-T.

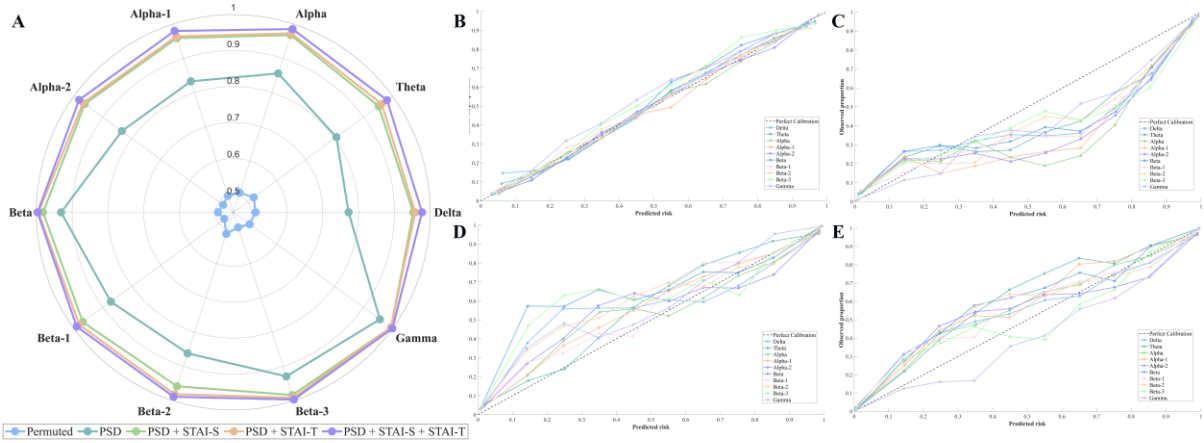

Figure 4 Classifier performance. (**A**) Classifier discrimination performance (AUC) across frequency bands for FM and HC. Calibration curves per frequency band for (**B**) PSD, (**C**) PSD + STAI-S, (**D**) PSD + STAI-T, and (**E**) PSD + STAI-S + STAI-T.

3.3.2 Classifying STFM and LTFM using EEG features

To compare short-term fibromyalgia (STFM) and long-term fibromyalgia (LTFM) groups, power spectral density (PSD) from EEG data was used to train a linear discriminant analysis (LDA) model. Model performance is shown in Figure 5 and further detailed in Supplementary Table 6. The model successfully distinguished STFM from LTFM patients, particularly in beta-1 (*ACC* = 0.87, *AUC* = 0.94), beta-2 (*ACC* = 0.87, *AUC* = 0.94), beta-3 (*ACC* = 0.94, *AUC* = 0.98), and gamma (*ACC* = 0.96, *AUC* = 0.99) bands. Calibration curves

were generally stable and close to the ideal diagonal, although beta, beta-3, and gamma bands exhibited greater deviations.

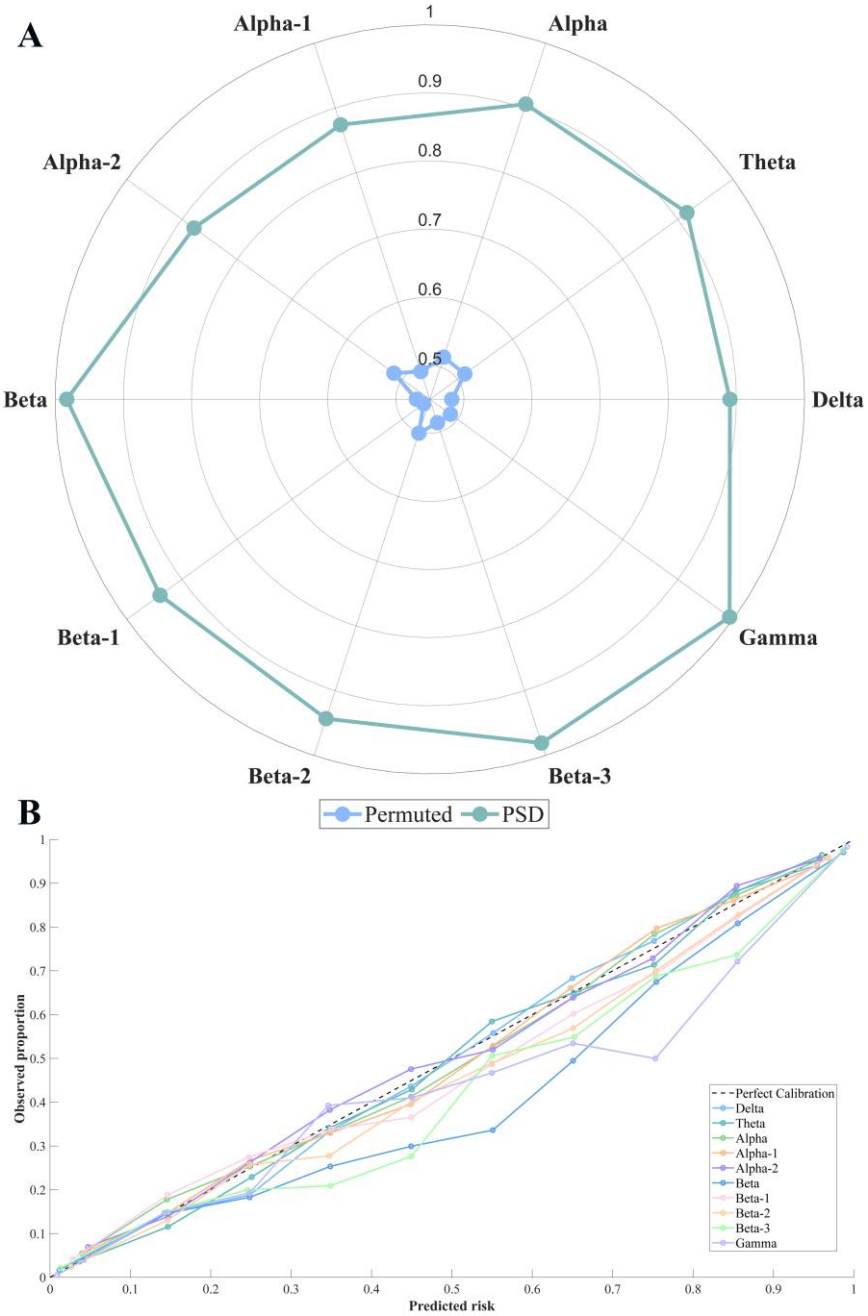

Figure 5. Classifier performance. (**A**) Classifier discrimination performance (AUC) across frequency bands for STFM and LTFM. (**B**) Calibration curves per frequency band using PSD values.

3.3.3 Channel contribution to group classification

To interpret the neural scalp sites contributing to classification, the correction method proposed by Haufe et al. [29] was applied to the weight matrix obtained after classification.

This transformation provides a more accurate spatial representation of relevant neural activity across frequency bands distinguishing FM from HC, as well as STFM from LTFM. The corrected weight maps are shown in Figure 6, and detailed in Supplementary Tables 7 and 8. In both comparisons, delta through alpha bands exhibited similar spatial patterns primarily in prefrontal regions. In the STFM and LTFM comparison, occipitotemporal regions also showed notable contributions. For beta through gamma bands, the FM and HC comparison revealed similar activity patterns in prefrontal, frontal, and temporoparietal regions. In contrast, the STFM and LTFM comparison highlighted significant contributions in temporal and frontal regions for beta and gamma bands, with additional involvement of parieto-occipital areas specifically for beta-3 and gamma.

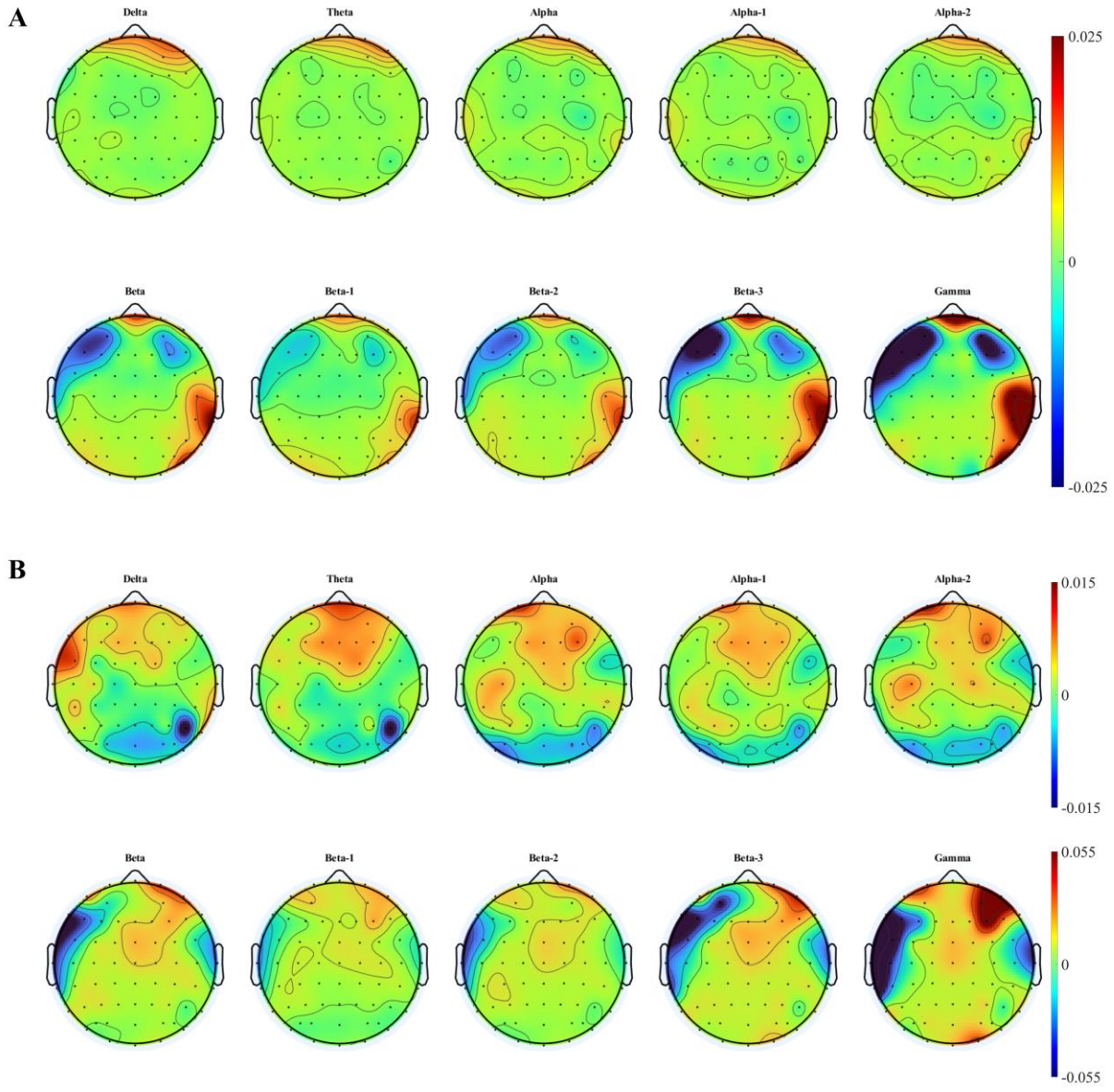

Figure 6 Topographic distribution of scalp site contributions across frequency bands. (**A**) Scalp site contributions in FM and HC. (**B**) Scalp site contributions in STFM and LTFM.

3.4 Medication effects on brain activity in the FM group

To assess potential medication effects on brain activity in FM patients, we conducted nonparametric permutation tests comparing mean power spectral density (PSD) values between medicated and non-medicated patients. Channels showing significant differences (i.e., $p < 0.05$) are illustrated in Figure 7 and detailed in Supplementary Table 9. Among

these, Fpz and Fp2 in the delta band for the antidepressants condition, as well as P6 in delta, F5 and F7 in beta-3 and gamma, and AF7 and F3 in gamma for the analgesics condition, contributed meaningfully to the classification models. While these effects were generally limited to isolated channels and did not indicate widespread alterations, the gamma band showed multiple frontal channels affected. For anxiolytics and antiepileptics/psycholeptics conditions, sample sizes (6 and 4 participants, respectively) were too small to conduct meaningful statistical analyses.

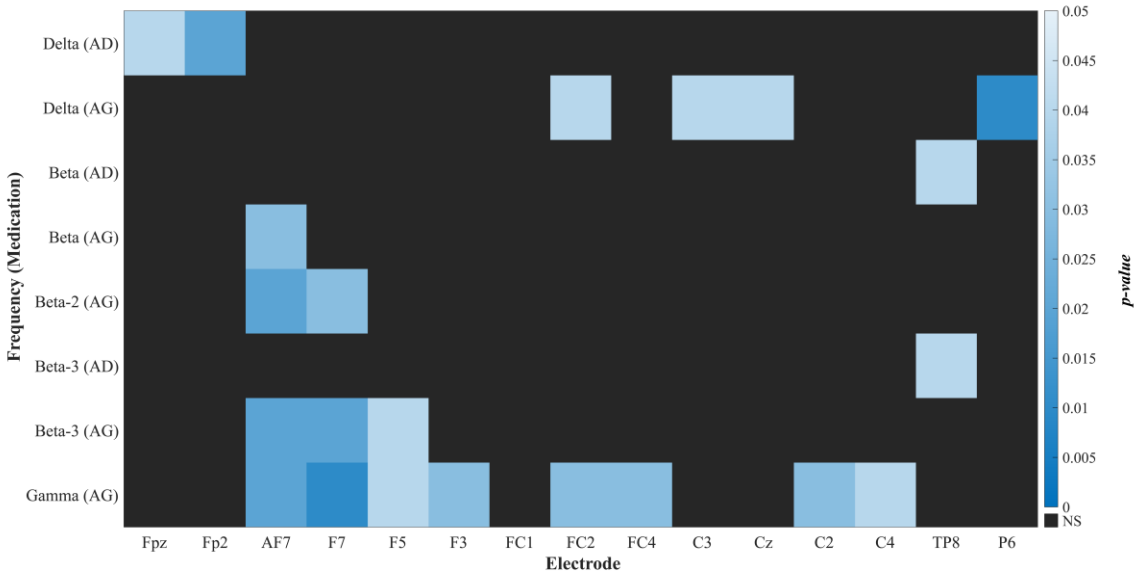

Figure 7 Heatmap of statistical differences in mean PSD values across frequency bands. Comparison between FM participants with and without medication use. Abbreviations: NS = Not Significant, AD = Antidepressants, AG = Analgesics.

4 Discussion

In the present study, we investigated abnormalities in EEG activity in fibromyalgia (FM) patients during open-eyes resting-state (RS). We applied a linear discriminant analysis (LDA) model in three novel analyses. First, we trained the model with power spectral density (PSD) and anxiety scores to distinguish FM patients from healthy controls (HC). Second, we used diagnosis duration to distinguish between short-term (STFM) and long-term FM (LTFM)

patients. Both analyses accurately differentiated groups across frequency bands. Third, we identified key scalp regions whose neural activity contributed most to the classification. This approach integrated EEG and psychometric data, linking brain activity to symptom duration and anxiety. By aligning our methodology with the study's objectives, we were able to highlight the critical role these variables play in understanding the heterogeneity and complexity of FM.

Building on our integrated approach, we identified specific neural features enabling accurate classification of FM patients and HC. Notably, beta and gamma frequency bands emerged as the most discriminative. Within the beta band, particularly beta-3, classification performance was strongest, with scalp key contributions over bilateral frontal, right temporal, and right parieto-occipital regions. As the analysis was conducted in sensor space rather than source space, cortical interpretations should be done carefully. Nonetheless, brain areas situated under these scalp locations, such as the anterior insular, dorsolateral prefrontal, and secondary somatosensory cortices have been implicated in pain perception and its modulation [2,26,58]. Moreover, beta-3 activity has been linked to interactions between sensory, affective, and attentional circuits involved in pain processing [2]. Abnormal beta oscillations have been linked not only to pain processing but also to impairments in motor control, visual attention, and emotion regulation [3,4,16,27]. While research on gamma activity in nociplastic pain is limited, increased gamma oscillations have been associated with heightened pain sensitivity and enhanced attentional focus on somatosensory stimuli [2,28,56].

Although beta oscillations relate to pain processing and broader cognitive functions, alpha and theta bands are more directly linked to pain inhibition and cognitive control [17,58]. Specifically, previous studies report a negative correlation between pain levels and alpha power, indicating that chronic pain in FM patients may act as a persistent noxious stimulus

that progressively diminishes alpha activity [42,58]. This aligns with our findings, where prefrontal regions exhibited strong positive weights contributing significantly to the classification of FM patients. Additionally, increased prefrontal theta PSD in FM might indicate diminished inhibitory control over pain processing. This dysregulation could contribute to maladaptive feedback loops in which pain is amplified and poorly modulated, as brain areas near these scalp locations, such as the dorsolateral prefrontal and medial prefrontal cortices, are involved in these processes [17,31].

In addition to pain-related symptoms, emotional symptoms such as anxiety are common in FM patients and often more severe than in age-matched controls, contributing to reduced quality of life [8,9,30]. Consistent with recent studies involving heat pain [32], our model's performance improved greatly when combining either state or trait anxiety with PSD, achieving the highest accuracy when both anxiety scores were included. Notably, combining trait anxiety with PSD outperformed the combination of state anxiety with PSD. This aligns with previous research suggesting that although both state and trait anxiety can intensify pain perception in FM patients, trait anxiety shows a stronger association [23]. These findings highlight that integrating psychological and electrophysiological variables provides a more comprehensive understanding of FM by capturing both emotional and neural profiles, offering deeper insight than analyzing each independently.

Evidence from FM and other chronic pain conditions suggests that prolonged exposure to pain alters brain structures and disrupts functional connectivity [3–5,35,37,44,51]. Although determining symptom onset in FM is challenging, as diagnosis often occurs years after initial symptoms, EEG studies associate longer symptom duration with more pronounced neural alterations [2]. This is consistent with our finding of high classification accuracy across all frequency bands when comparing STFM and LTFM groups. Additionally, altered theta power within frontal, frontocentral, and parietal regions has been associated with ongoing

tonic pain and fatigue in FM [17,59]. In our study, weights revealed strong contributions from frontal and frontocentral regions to the classification of the STFM group, while parietal regions contributed more substantially to the LTFM group. Regarding other frequency bands, the observed patterns may indicate exacerbations due to prolonged exposure to FM symptoms in the same regions commonly affected in FM when compared to HC, particularly those involved in pain processing and cognitive control.

The current study has several potential limitations. Other contributing factors cannot be ruled out, and further research is needed to clarify these findings. For instance, although the channels showing significant differences did not substantially influence classification models, and analgesic use has not been reported to affect pain-related brain activity, its impact cannot be entirely dismissed. Additionally, while some results align with prior univariate studies, several key regions within specific frequency bands remain underexplored, prompting further investigation to better understand their role in FM-related neurophysiological alterations. Finally, although task-related activity was carefully removed, the possibility of residual confounds remains, supporting the need for future studies employing true RS-EEG data.

In sum, our findings reveal significant differences in RS-EEG activity between FM patients and HC, as well as between STFM and LTFM. Incorporating anxiety scores improved the model's discriminative ability, emphasizing the value of integrating both emotional and neural factors. Frequency-specific alterations, particularly in scalp regions consistently associated with pain processing and cognitive control, support the notion that FM involves disrupted neural mechanisms of pain. Furthermore, multivariate pattern analysis effectively addresses the research questions, providing deeper insights into the disorder's complexity. Building on prior work using traditional methods, this approach provides a clearer picture of the neural alterations associated with FM. Given the ease of acquiring RS-EEG in clinical settings, it may be valuable for clinicians and researchers to consider focusing on frequency

bands that show the most promise in classification, such as beta and gamma bands. This could help advance the development of EEG based biomarkers for FM, ultimately improving diagnostic and therapeutic strategies for the disease.

5 Funding statement

This work was supported by grant PID2020-115463RB-I00 from the Ministerio de Ciencia e Innovación of Spain.

6 Data availability statement

The data supporting the findings of this study are available in the OSF repository at https://osf.io/gyk89/

7 Conflict of Interest statement

The authors have no conflicts of interest to declare.

8 References

[1] Abdellatef E, Emara HM, Shoaib MR, Ibrahim FE, Elwekeil M, El-Shafai W, Taha TE, El-Fishawy AS, El-Rabaie E-SM, Eldokany IM, Abd El-Samie FE. Automated diagnosis of EEG abnormalities with different classification techniques. Med Biol Eng Comput 2023;61:3363–3385.

[2] Alves RL, Zortea M, Serrano PV, Brugnera Tomedi R, Pereira De Almeida R, Torres ILS, Fregni F, Caumo W. High-beta oscillations at EEG resting state and hyperconnectivity of pain circuitry in fibromyalgia: an exploratory cross-sectional study. Front Neurosci 2023;17:1233979.

[3] Apkarian AV, Sosa Y, Sonty S, Levy RM, Harden RN, Parrish TB, Gitelman DR. Chronic Back Pain Is Associated with Decreased Prefrontal and Thalamic Gray Matter Density. J Neurosci 2004;24:10410–10415.

[4] Baliki MN, Geha PY, Apkarian AV, Chialvo DR. Beyond Feeling: Chronic Pain Hurts the Brain, Disrupting the Default-Mode Network Dynamics. J Neurosci 2008;28:1398–1403.

[5] Bekkelund SI, Pierre-Jerome C, Husby G, Mellgren SI. Quantitative cerebral MR in rheumatoid arthritis. AJNR Am J Neuroradiol 1995;16:767–772.

[6] Blankertz B, Lemm S, Treder M, Haufe S, Müller K-R. Single-trial analysis and classification of ERP components — A tutorial. NeuroImage 2011;56:814–825.

[7] Carretié L. Exogenous (automatic) attention to emotional stimuli: a review. Cogn Affect Behav Neurosci 2014;14:1228–1258.

[8] Catalá P, Gutiérrez L, Écija C, Peñacoba C. Pathological Cycle between Pain, Insomnia, and Anxiety in Women with Fibromyalgia and its Association with Disease Impact. Biomedicines 2023;11:148.

[9] Cetingok S, Seker O, Cetingok H. The relationship between fibromyalgia and depression, anxiety, anxiety sensitivity, fear avoidance beliefs, and quality of life in female patients. Medicine 2022;101:e30868.

[10] Choe MK, Lim M, Kim JS, Lee DS, Chung CK. Disrupted Resting State Network of Fibromyalgia in Theta frequency. Sci Rep 2018;8:2064.

[11] Clauw DJ. Fibromyalgia: A Clinical Review. JAMA 2014;311:1547.

[12] Clauw DJ. From fibrositis to fibromyalgia to nociplastic pain: how rheumatology helped get us here and where do we go from here? Annals of the Rheumatic Diseases 2024;83:1421–1427.

[13] Cortes C, Vapnik V. Support-vector networks. Mach Learn 1995;20:273–297.

[14] D'Croz-Baron DF, Bréchet L, Baker M, Karp T. Auditory and Visual Tasks Influence the Temporal Dynamics of EEG Microstates During Post-encoding Rest. Brain Topogr 2021;34:19–28.

[15] Delorme A, Makeig S. EEGLAB: an open source toolbox for analysis of single-trial EEG dynamics including independent component analysis. Journal of Neuroscience Methods 2004;134:9–21.

[16] Engel AK, Fries P. Beta-band oscillations — signalling the status quo? Current Opinion in Neurobiology 2010;20:156–165.

[17] Fallon N, Chiu Y, Nurmikko T, Stancak A. Altered theta oscillations in resting EEG of fibromyalgia syndrome patients. European Journal of Pain 2018;22:49–57.

[18] Fernandes-Magalhaes R, Carpio A, Ferrera D, Peláez I, De Lahoz ME, Van Ryckeghem D, Van Damme S, Mercado F. Neural mechanisms underlying attentional bias modification in fibromyalgia patients: a double-blind ERP study. Eur Arch Psychiatry Clin Neurosci 2024;274:1197–1213.

[19] Fernandes-Magalhaes R, Ferrera D, Peláez I, Martín-Buro MC, Carpio A, De Lahoz ME, Barjola P, Mercado F. Neural correlates of the attentional bias towards pain-related faces in fibromyalgia patients: An ERP study using a dot-probe task. Neuropsychologia 2022;166:108141.

[20] Ferrera D, Gómez-Esquer F, Peláez I, Barjola P, Fernandes-Magalhaes R, Carpio A, De Lahoz ME, Díaz-Gil G, Mercado F. Effects of COMT Genotypes on Working Memory Performance in Fibromyalgia Patients. JCM 2020;9:2479.

[21] Ferrera D, Mercado F, Peláez I, Martínez-Iñigo D, Fernandes-Magalhaes R, Barjola P, Écija C, Díaz-Gil G, Gómez-Esquer F. Fear of pain moderates the relationship between self-reported fatigue and methionine allele of catechol-O-methyltransferase gene in patients with fibromyalgia. PLoS ONE 2021;16:e0250547.

[22] Fitzcharles M-A, Cohen SP, Clauw DJ, Littlejohn G, Usui C, Häuser W. Nociplastic pain: towards an understanding of prevalent pain conditions. The Lancet 2021;397:2098–2110.

[23] Galvez-Sánchez CM, Montoro CI, Duschek S, Reyes Del Paso GA. Depression and trait-anxiety mediate the influence of clinical pain on health-related quality of life in fibromyalgia. Journal of Affective Disorders 2020;265:486–495.

[24] Garrett D, Peterson DA, Anderson CW, Thaut MH. Comparison of linear, nonlinear, and feature selection methods for EEG signal classification. IEEE Trans Neural Syst Rehabil Eng 2003;11:141–144.

[25] Giorgi V, Sirotti S, Romano ME, Marotto D, Ablin JN, Salaffi F, Sarzi-Puttini P. Review Fibromyalgia: one year in review 2022. Clinical and Experimental Rheumatology 2022.

[26] González-Villar AJ, Triñanes Y, Gómez-Perretta C, Carrillo-de-la-Peña MT. Patients with fibromyalgia show increased beta connectivity across distant networks and microstates alterations in resting-state electroencephalogram. NeuroImage 2020;223:117266.

[27] Hauck M, Domnick C, Lorenz J, Gerloff C, Engel AK. Top-down and bottom-up modulation of pain-induced oscillations. Front Hum Neurosci 2015;9. doi:10.3389/fnhum.2015.00375.

[28] Hauck M, Lorenz J, Engel AK. Attention to Painful Stimulation Enhances γ-Band Activity and Synchronization in Human Sensorimotor Cortex. J Neurosci 2007;27:9270–9277.

[29] Haufe S, Meinecke F, Görgen K, Dähne S, Haynes J-D, Blankertz B, Bießmann F. On the interpretation of weight vectors of linear models in multivariate neuroimaging. NeuroImage 2014;87:96–110.

[30] Henao-Pérez M, López-Medina DC, Arboleda A, Bedoya Monsalve S, Zea JA. Patients With Fibromyalgia, Depression, and/or Anxiety and Sex Differences. Am J Mens Health 2022;16:15579883221110351.

[31] Henderson LA, Peck CC, Petersen ET, Rae CD, Youssef AM, Reeves JM, Wilcox SL, Akhter R, Murray GM, Gustin SM. Chronic Pain: Lost Inhibition? J Neurosci 2013;33:7574–7582.

[32] Hsiao F-J, Chen W-T, Pan L-LH, Liu H-Y, Wang Y-F, Chen S-P, Lai K-L, Wang S-J. Machine learning–based prediction of heat pain sensitivity by using resting-state EEG. Front Biosci (Landmark Ed) 2021;26:1537–1547.

[33] Hsiao F-J, Wang S-J, Lin Y-Y, Fuh J-L, Ko Y-C, Wang P-N, Chen W-T. Altered insula–default mode network connectivity in fibromyalgia: a resting-state magnetoencephalographic study. J Headache Pain 2017;18:89.

[34] Iemi L, Busch NA, Laudini A, Haegens S, Samaha J, Villringer A, Nikulin VV. Multiple mechanisms link prestimulus neural oscillations to sensory responses. eLife 2019;8:e43620.

[35] Jin C, Yuan K, Zhao L, Zhao L, Yu D, Von Deneen KM, Zhang M, Qin W, Sun W, Tian J. Structural and functional abnormalities in migraine patients without aura. NMR in Biomedicine 2013;26:58–64.

[36] Khanam F, Hossain ABMA, Ahmad M. Electroencephalogram-based cognitive load level classification using wavelet decomposition and support vector machine. Brain-Computer Interfaces 2023;10:1–15.

[37] Kuchinad A, Schweinhardt P, Seminowicz DA, Wood PB, Chizh BA, Bushnell MC. Accelerated Brain Gray Matter Loss in Fibromyalgia Patients: Premature Aging of the Brain? J Neurosci 2007;27:4004–4007.

[38] Kumbhare D, Ahmed S, Watter S. A narrative review on the difficulties associated with fibromyalgia diagnosis. Therapeutic Advances in Musculoskeletal 2018;10:13–26.

[39] López-García D, Peñalver JMG, Górriz JM, Ruz M. MVPAlab: A machine learning decoding toolbox for multidimensional electroencephalography data. Computer Methods and Programs in Biomedicine 2022;214:106549.

[40] López-Solà M, Woo C-W, Pujol J, Deus J, Harrison BJ, Monfort J, Wager TD. Towards a neurophysiological signature for fibromyalgia. Pain 2017;158:34–47.

[41] Maris E, Oostenveld R. Nonparametric statistical testing of EEG- and MEG-data. Journal of Neuroscience Methods 2007;164:177–190.

[42] Martín-Brufau R, Gómez MN, Sanchez-Sanchez-Rojas L, Nombela C. Fibromyalgia Detection Based on EEG Connectivity Patterns. JCM 2021;10:3277.

[43] MATLAB. 2023. Available: https://www.mathworks.com/.

[44] McCrae C, O'Shea A, Boissoneault J, Vatthauer K, Robinson M, Staud R, Perlstein W, Craggs J. Fibromyalgia patients have reduced hippocampal volume compared with healthy controls. JPR 2015:47.

[45] Moons KGM, Damen JAA, Kaul T, Hooft L, Andaur Navarro C, Dhiman P, Beam AL, Van Calster B, Celi LA, Denaxas S, Denniston AK, Ghassemi M, Heinze G, Kengne AP, Maier-Hein L, Liu X, Logullo P, McCradden MD, Liu N, Oakden-Rayner L, Singh K, Ting DS, Wynants L, Yang B, Reitsma JB, Riley RD, Collins GS, Van Smeden M. PROBAST+AI: an updated quality, risk of bias, and applicability assessment tool for

prediction models using regression or artificial intelligence methods. BMJ 2025:e082505.

[46] On behalf of Topic Group 'Evaluating diagnostic tests and prediction models' of the STRATOS initiative, Van Calster B, McLernon DJ, Van Smeden M, Wynants L, Steyerberg EW. Calibration: the Achilles heel of predictive analytics. BMC Med 2019;17:230.

[47] Oostenveld R, Fries P, Maris E, Schoffelen J-M. FieldTrip: Open Source Software for Advanced Analysis of MEG, EEG, and Invasive Electrophysiological Data. Computational Intelligence and Neuroscience 2011;2011:1–9.

[48] Pujol J, Blanco-Hinojo L, Doreste A, Ojeda F, Martínez-Vilavella G, Pérez-Sola V, Deus J, Monfort J. Distinctive alterations in the functional anatomy of the cerebral cortex in pain-sensitized osteoarthritis and fibromyalgia patients. Arthritis Res Ther 2022;24:252.

[49] Pujol J, Macià D, Garcia-Fontanals A, Blanco-Hinojo L, López-Solà M, Garcia-Blanco S, Poca-Dias V, Harrison BJ, Contreras-Rodríguez O, Monfort J, Garcia-Fructuoso F, Deus J. The contribution of sensory system functional connectivity reduction to clinical pain in fibromyalgia. Pain 2014;155:1492–1503.

[50] Raichle ME, Snyder AZ. A default mode of brain function: A brief history of an evolving idea. NeuroImage 2007;37:1083–1090.

[51] Rodriguez-Raecke R, Niemeier A, Ihle K, Ruether W, May A. Structural Brain Changes in Chronic Pain Reflect Probably Neither Damage Nor Atrophy. PLoS ONE 2013;8:e54475.

[52] Ruiz De Miras J, Ibáñez-Molina AJ, Soriano MF, Iglesias-Parro S. Schizophrenia classification using machine learning on resting state EEG signal. Biomedical Signal Processing and Control 2023;79:104233.

[53] Saviola F, Pappaianni E, Monti A, Grecucci A, Jovicich J, De Pisapia N. Trait and state anxiety are mapped differently in the human brain. Sci Rep 2020;10:11112.

[54] Sha'abani MNAH, Fuad N, Jamal N, Ismail MF. kNN and SVM Classification for EEG: A Review. In: Kasruddin Nasir AN, Ahmad MA, Najib MS, Abdul Wahab Y, Othman NA, Abd Ghani NM, Irawan A, Khatun S, Raja Ismail RMT, Saari MM, Daud MR, Mohd Faudzi AA, editors. InECCE2019. Lecture Notes in Electrical Engineering. Singapore: Springer Singapore, 2020, Vol. 632. pp. 555–565. doi:10.1007/978-981-15-2317-5_47.

[55] Spielberger CD, Gorsuch RL, Lushene EE. Manual del Cuestionario de Ansiedad Estado/Rasgo (STAI). TEA Ediciones, Madrid 1982.

[56] Stefani LC, Leite FM, Da Graça L. Tarragó M, Zanette SA, De Souza A, Castro SM, Caumo W. BDNF and serum S100B levels according the spectrum of structural pathology in chronic pain patients. Neuroscience Letters 2019;706:105–109.

[57] Thanh Nhu N, Chen DY-T, Kang J-H. Identification of Resting-State Network Functional Connectivity and Brain Structural Signatures in Fibromyalgia Using a Machine Learning Approach. Biomedicines 2022;10:3002.

[58] Villafaina S, Collado-Mateo D, Fuentes-García JP. Impact of Fibromyalgia on Alpha-2 EEG Power Spectrum in the Resting Condition: A Descriptive Correlational Study. BioMed Research International 2019;2019:1–6.

[59] Villafaina S, Collado-Mateo D, Fuentes-García JP, Domínguez-Muñoz FJ, Gusi N. Duration of the Symptoms and Brain Aging in Women with Fibromyalgia: A Cross-Sectional Study. Applied Sciences 2019;9:2106.

[60] Walz JM, Goldman RI, Carapezza M, Muraskin J, Brown TR, Sajda P. Simultaneous EEG–fMRI reveals a temporal cascade of task-related and default-mode activations during a simple target detection task. NeuroImage 2014;102:229–239.

[61] Wolfe F, Clauw DJ, Fitzcharles M, Goldenberg DL, Katz RS, Mease P, Russell AS, Russell IJ, Winfield JB, Yunus MB. The American College of Rheumatology Preliminary Diagnostic Criteria for Fibromyalgia and Measurement of Symptom Severity. Arthritis Care & Research 2010;62:600–610.

[62] Wolfe F, Clauw DJ, Fitzcharles M-A, Goldenberg DL, Häuser W, Katz RL, Mease PJ, Russell AS, Russell IJ, Walitt B. 2016 Revisions to the 2010/2011 fibromyalgia diagnostic criteria. Seminars in Arthritis and Rheumatism 2016;46:319–329.

[63] Wolfe F, Smythe HA, Yunus MB, Bennett RM, Bombardier C, Goldenberg DL, Tugwell P, Campbell SM, Abeles M, Clark P, Fam AG, Farber SJ, Fiechtner JJ, Michael Franklin C, Gatter RA, Hamaty D, Lessard J, Lichtbroun AS, Masi AT, Mccain GA, John Reynolds W, Romano TJ, Jon Russell I, Sheon RP. The american college of rheumatology 1990 criteria for the classification of fibromyalgia. Arthritis & Rheumatism 1990;33:160–172.

[64] Yu C, Wang M. Survey of emotion recognition methods using EEG information. Cognitive Robotics 2022;2:132–146.

[65] Zafar R, Kamel N, Naufal M, Malik AS, Dass SC, Ahmad RF, Abdullah JM, Reza F. A study of decoding human brain activities from simultaneous data of EEG and fMRI using MVPA. Australas Phys Eng Sci Med 2018;41:633–645.

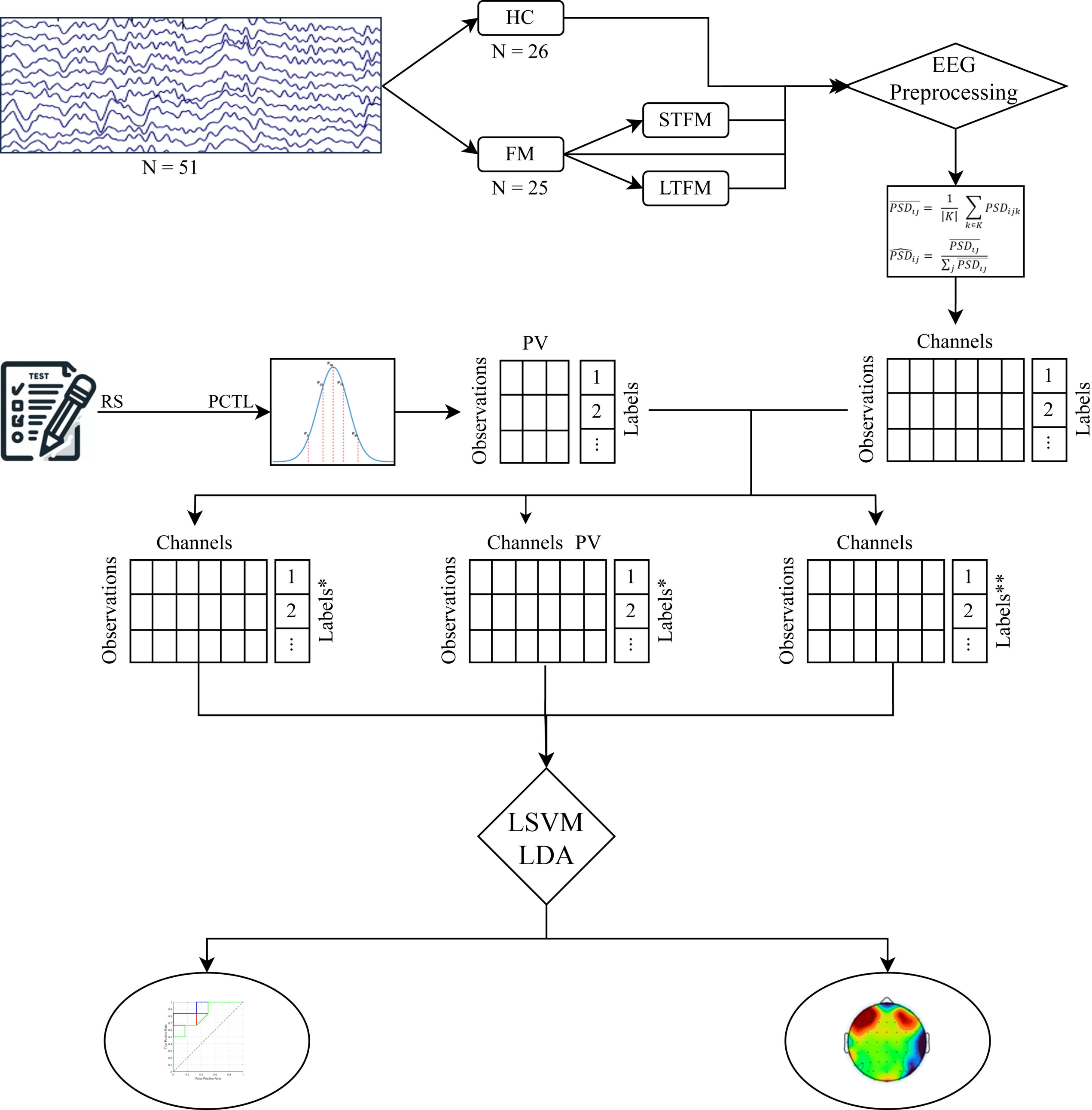
N = 51
HC
N = 26
FM
N = 25
STFM
LTFM
EEG Preprocessing
$\overline{PSD_{ij}} = \frac{1}{|K|} \sum_{k \in K} PSD_{ijk}$
$\widehat{PSD_{ij}} = \frac{\overline{PSD_{ij}}}{\sum_j \overline{PSD_{ij}}}$
Channels
TEST
RS
PCTL
PV
Observations
Labels
1
2
...
Channels
Observations
Labels
1
2
...
Channels
Observations
Labels*
1
2
...
Channels PV
Observations
Labels*
1
2
...
Channels
Observations
Labels**
1
2
...
LSVM
LDA

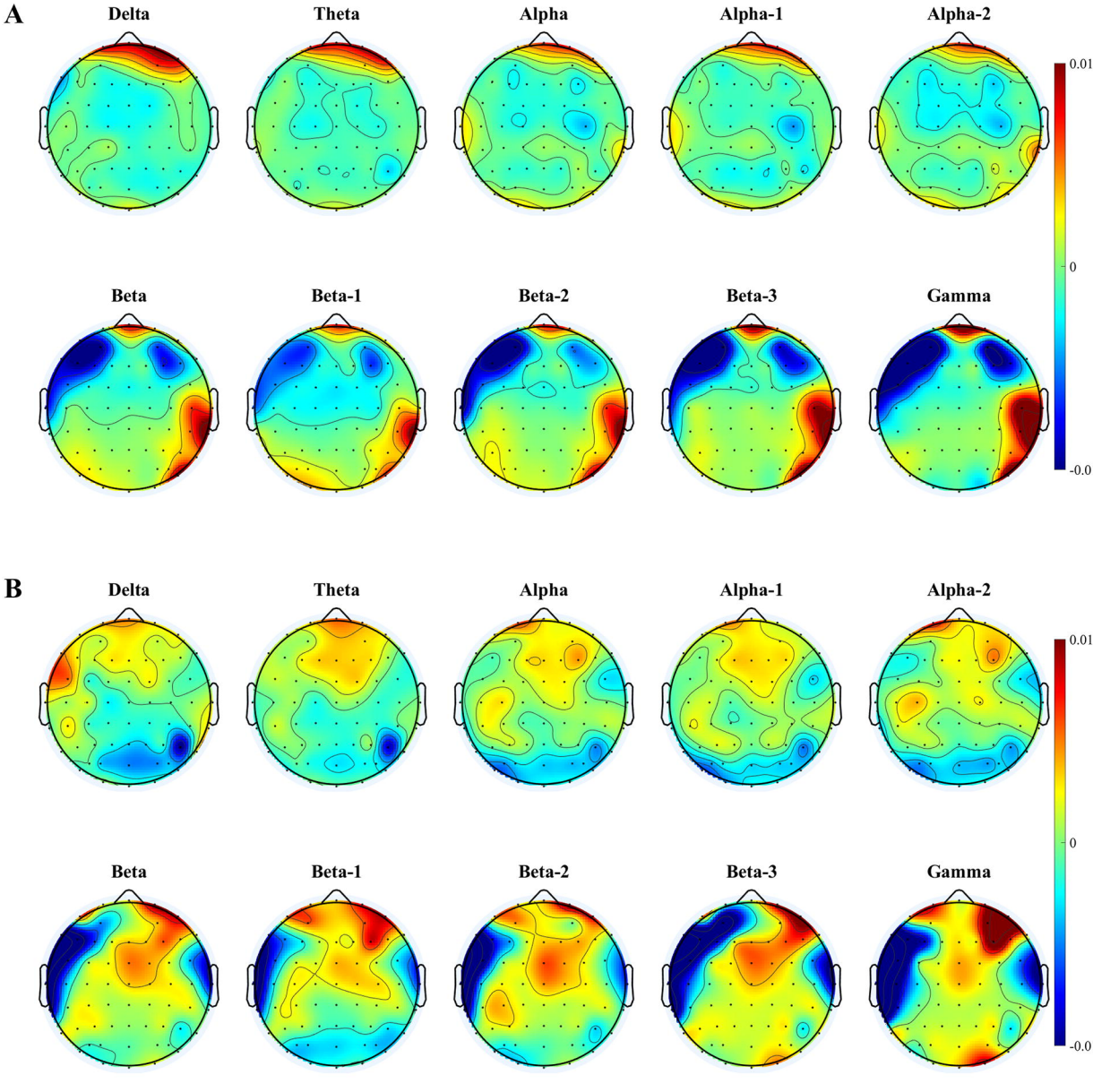
A
Delta
Theta
Alpha
Alpha-1
Alpha-2
Beta
Beta-1
Beta-2
Beta-3
Gamma
0.01
0
-0.01
B
Delta
Theta
Alpha
Alpha-1
Alpha-2
Beta
Beta-1
Beta-2
Beta-3
Gamma
0.01
0
-0.01

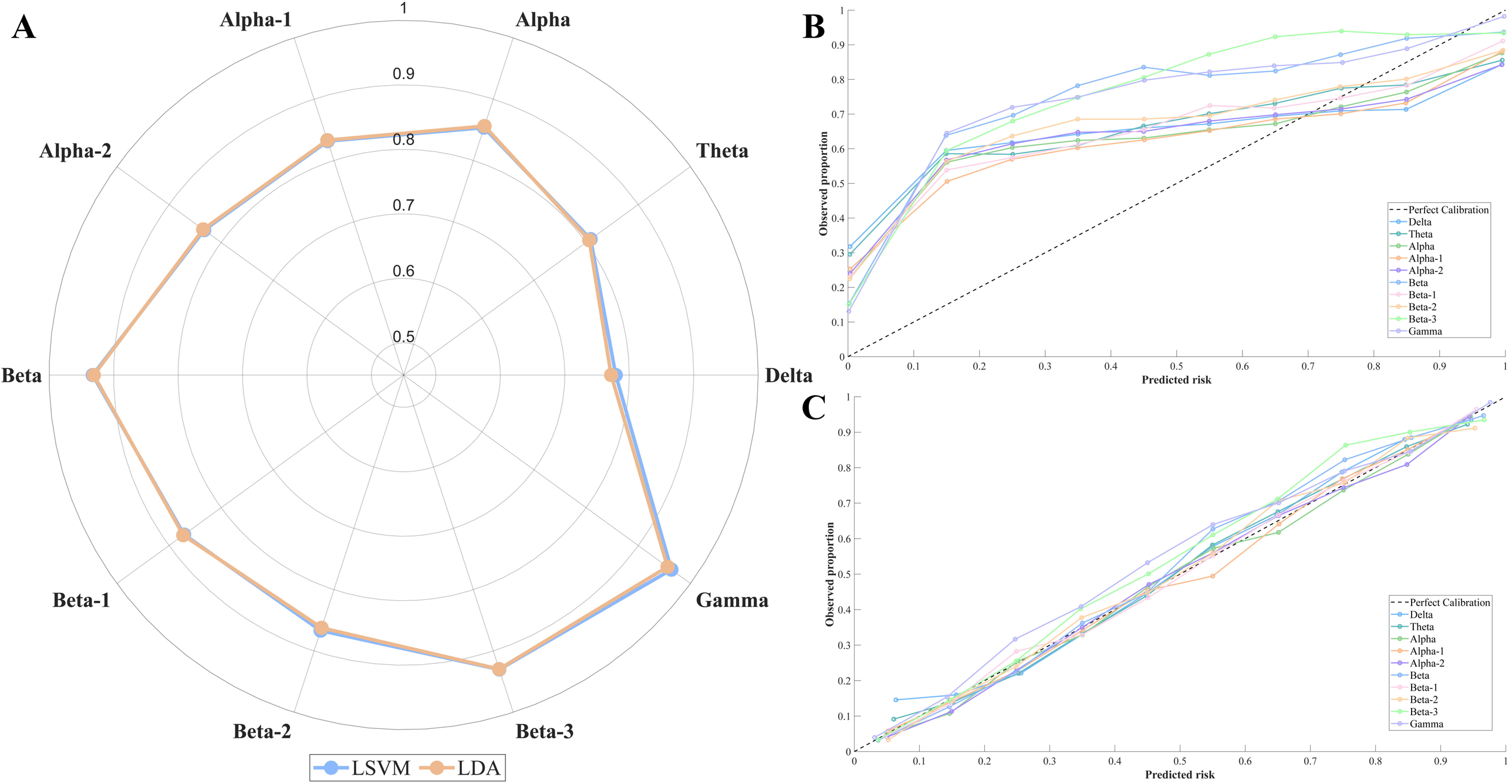
A
Alpha-1
Alpha
Alpha-2
Theta
Beta
Delta
Beta-1
Gamma
Beta-2
Beta-3
1
0.9
0.8
0.7
0.6
0.5
LSVM
LDA
B
Observed proportion
Predicted risk
Perfect Calibration
Delta
Theta
Alpha
Alpha-1
Alpha-2
Beta
Beta-1
Beta-2
Beta-3
Gamma
C
Observed proportion
Predicted risk
Perfect Calibration
Delta
Theta
Alpha
Alpha-1
Alpha-2
Beta
Beta-1
Beta-2
Beta-3
Gamma

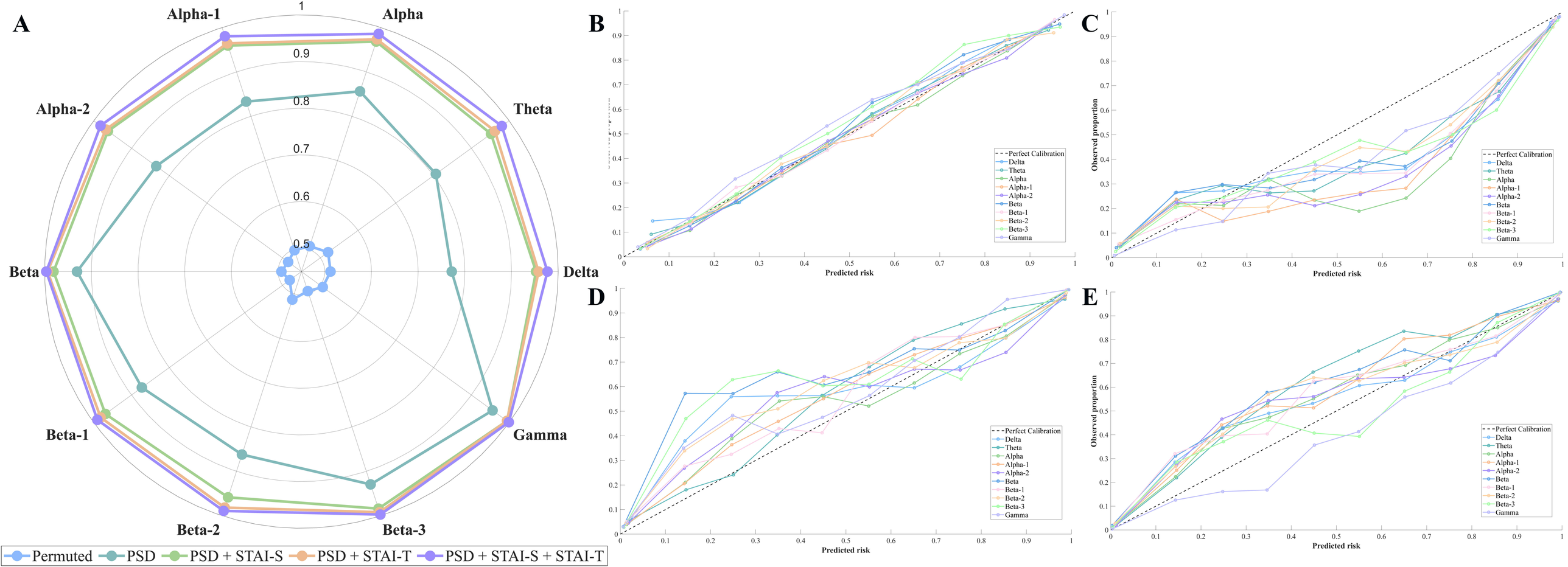
A
Alpha-1
Alpha
Alpha-2
Theta
Beta
Delta
Beta-1
Gamma
Beta-2
Beta-3
1
0.9
0.8
0.7
0.6
0.5
Permuted
PSD
PSD + STAI-S
PSD + STAI-T
PSD + STAI-S + STAI-T
B
C
D
E
Observed proportion
Predicted risk
Perfect Calibration
Delta
Theta
Alpha
Alpha-1
Alpha-2
Beta
Beta-1
Beta-2
Beta-3
Gamma

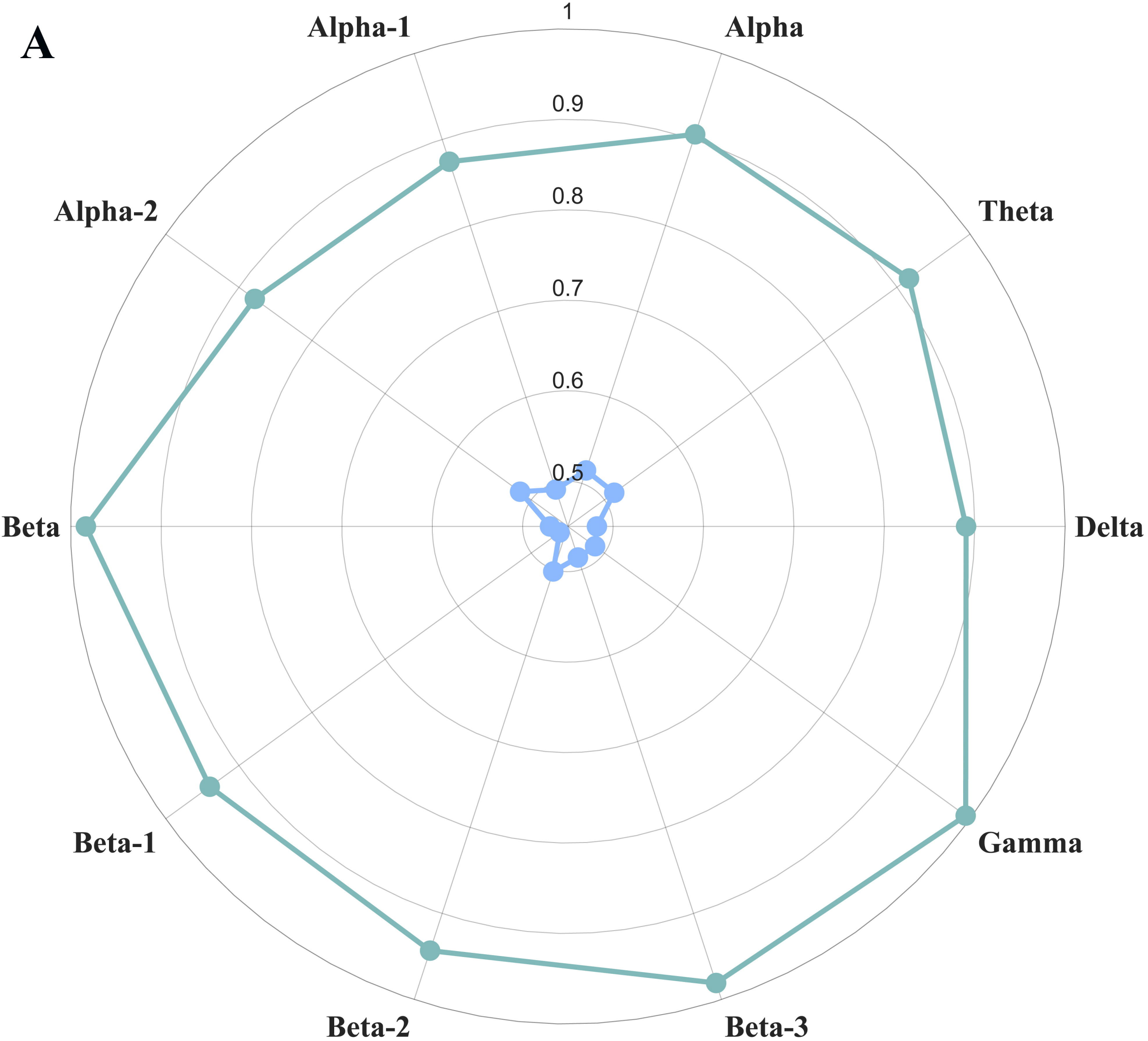
A
Alpha-1
Alpha
Alpha-2
Theta
Beta
Delta
Beta-1
Gamma
Beta-2
Beta-3
1
0.9
0.8
0.7
0.6
0.5

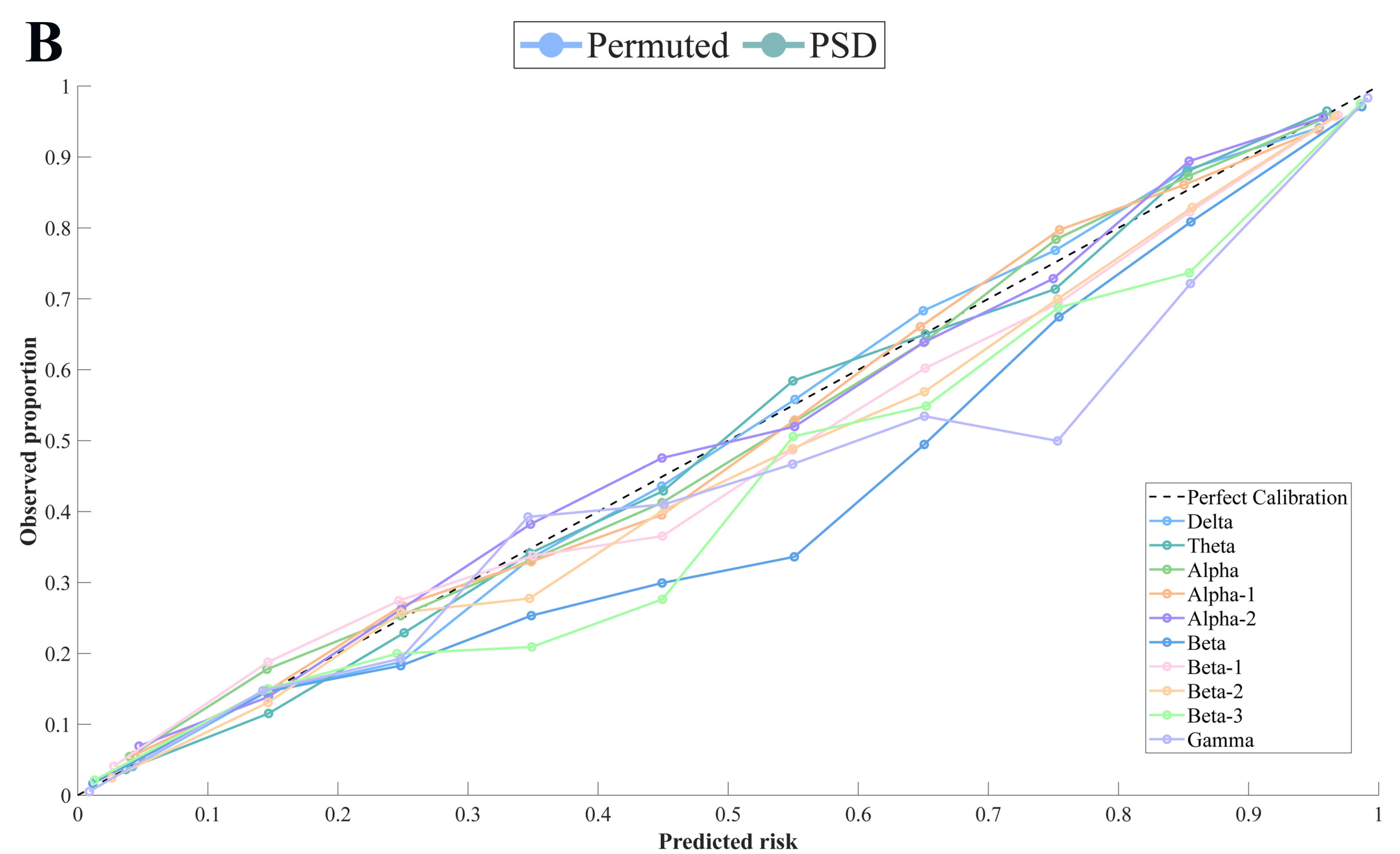
B
Permuted
PSD
Observed proportion
Predicted risk
0
0.1
0.2
0.3
0.4
0.5
0.6
0.7
0.8
0.9
1
Perfect Calibration
Delta
Theta
Alpha
Alpha-1
Alpha-2
Beta
Beta-1
Beta-2
Beta-3
Gamma

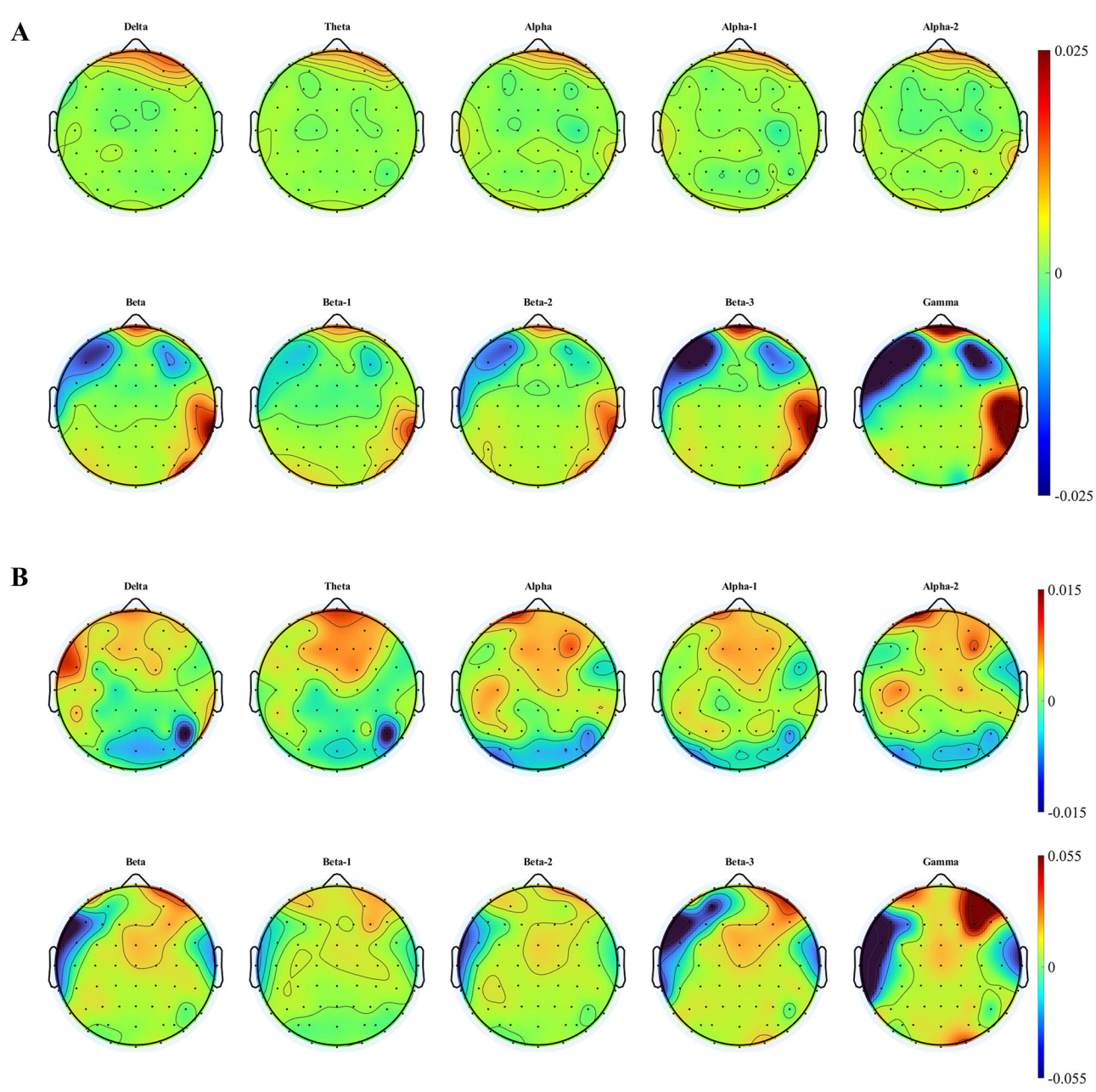
A
Delta
Theta
Alpha
Alpha-1
Alpha-2
Beta
Beta-1
Beta-2
Beta-3
Gamma
0.025
0
-0.025
B
Delta
Theta
Alpha
Alpha-1
Alpha-2
0.015
0
-0.015
Beta
Beta-1
Beta-2
Beta-3
Gamma
0.055
0
-0.055

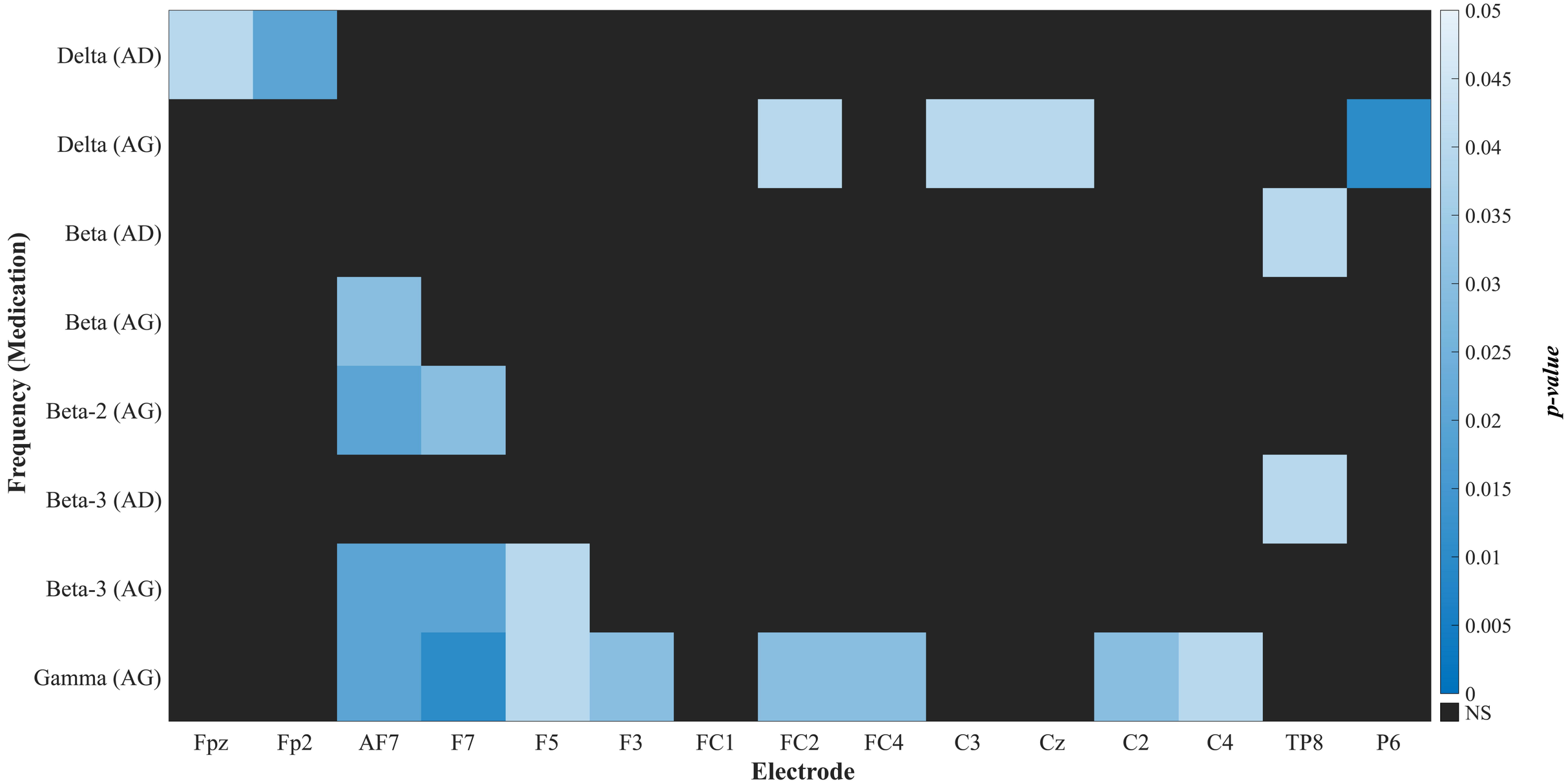
Frequency (Medication)
Delta (AD)
Delta (AG)
Beta (AD)
Beta (AG)
Beta-2 (AG)
Beta-3 (AD)
Beta-3 (AG)
Gamma (AG)
Fpz
Fp2
AF7
F7
F5
F3
FC1
FC2
FC4
C3
Cz
C2
C4
TP8
P6
Electrode
0.05
0.045
0.04
0.035
0.03
0.025
0.02
0.015
0.01
0.005
0
NS
p-value